Finite Element Approximation and Input Parameterization for the Optimal Control of Current Profiles in Tokamak Plasmas *

Zhigang Ren * Chao Xu * Qun Lin ** Ryan Loxton ** Kok Lay Teo ** Jian Chu *

* *The State Key Laboratory of Industrial Control Technology and Institute of Cyber-Systems & Control, Zhejiang University, Hangzhou, Zhejiang, China (e-mail: renzhigang@zju.edu.cn, cxu@zju.edu.cn, chuj@csc.zju.edu.cn)*
** *Department of Mathematics & Statistics, Curtin University, Perth, Western Australia, Australia (e-mail: q.lin@curtin.edu.au, r.loxton@curtin.edu.au, k.l.teo@curtin.edu.au)*

Abstract: In this paper, we consider a simplified dynamic model describing the evolution of the poloidal flux during the ramp-up phase of the tokamak discharge. We first use the Galerkin method to obtain a finite-dimensional model based on the original PDE system. Then, we apply the control parameterization method to obtain an approximate optimal parameter selection problem governed by a lumped parameter system. Computational optimization techniques are subsequently deployed to solve this approximate problem. To validate our approach, we perform numerical simulations using experimental data from the DIII-D tokamak in San Diego, California. The results show that our numerical optimization procedure can generate optimal controls that drive the current profile to within close proximity of the desired profile at the terminal time, thus demonstrating that the Galerkin and control parameterization methods are effective tools for current profile control in tokamak plasmas.

Keywords: Nuclear Fusion, Current Profile Control, Galerkin Method, Control Parameterization, Sequential Quadratic Programming (SQP)

1. INTRODUCTION

Control engineering is considered one of the three critical technologies for achieving viable nuclear fusion power. [1] Accordingly, it has become an important area for multidisciplinary collaboration in the fusion research community. Many exciting research topics from the viewpoint of control engineering are surveyed in the book by Ariola and Pironti (2008) and two special issues of IEEE Control Systems Magazine [2]. Among many challenging research issues, the control of the current profile in tokamak plasmas is known to be critical to improved confinement, enhanced magnetohydrodynamic stability and effective steady-state operation (see Murakami et al. (2006) and Taylor (1997)). The evolution in time of the current profile is related to the evolution of the poloidal magnetic flux, which is modeled by the magnetic diffusion equation, a parabolic partial differential equation (PDE) in the normalized cylindrical coordinate system. The problem of manipulating the current profile to achieve high-performance while satisfying safety requirements has attracted considerable attention in the literature.

In Witrant et al. (2007) and Ou et al. (2007), this problem was formulated mathematically using a distributed parameter system framework. In our current work, using the same framework proposed by Witrant et al. (2007) and Ou et al. (2007), we consider the problem of attaining the best possible approximate matching at the final time T during the early flat-top phase of the plasma current pulse, as shown in Fig. 1. This problem can be formulated as a finite-time optimal control problem for the magnetic flux diffusion PDE system, which can be considered as a bilinear infinite-dimensional system, i.e., the diffusivity control term appears in the second-order elliptic operator. In Ou et al. (2008), the extremum seeking approach proposed by Ariyur and Krstic (2003) is used to compute the optimal open-loop control trajectory during the ramp-up phase of the plasma discharge. This approach can handle quite complicated constraints without being trapped in local minima. A reduced-order model is obtained in Xu et al. (2010) by using the proper orthogonal decomposition (POD) method, which can reduce the computational burden of the extremum seeking approach in Ou et al. (2008) and make receding horizon control a feasible approach for future work (Ou et al. (2011)).

[1] E. Synakowski's presentation titled Fusion Energy Research: On Our Science, Leverage and Credibility at the University Fusion Association General Meeting, held during the 51st Annual Meeting of the American Physical Society Division of Plasma Physics (November 2-6, 2009, Atlanta, Georgia, USA).
[2] Refer to papers in the special issues titled "Control of Tokamak Plasmas: Part I" (October 2005) and "Control of Tokamak Plasmas: Part II" (April 2006) in IEEE Control Systems Magazine, organized by A. Pironti and M. Walker.
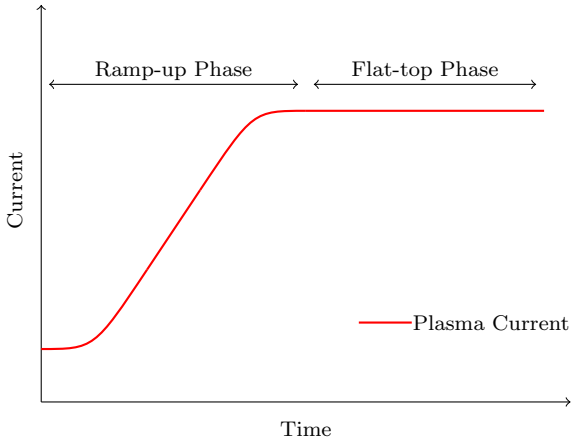
Fig. 1. The plasma current evolution can be divided into two phases – ramp-up phase and flat-top phase.

In this paper, we consider the same open-loop optimal control problem as in Ou et al. (2008) and Xu et al. (2010), but we solve it using a different approach. We first discretize the model over the state space using the finite element method (FEM), rather than the POD method, to yield a finite-dimensional system of ordinary differential equations (ODEs). The motivation for performing this discretization procedure is that, in general, it is much easier to solve the approximate finite-dimensional optimal control problem than the original infinite-dimensional problem governed by PDEs. After using FEM to obtain a finite-dimensional system of ODEs, we then apply the control parameterization approach to obtain an optimal parameter selection problem (Teo et al. (1991)). This involves approximating the control function by a linear combination of temporal basis functions (usually simple characteristic functions, polynomials or splines) with the constant coefficients to be determined by numerical optimization procedures such as sequential quadratic programming (SQP). This methodology follows the *discretize-then-control* approach rather than the alternative approach of *control-then-discretize*. The numerical convergence of suboptimal controls generated by the discretize-then-control approach remains a challenging issue, much more difficult than the convergence analysis for the numerical discretization of PDEs. See Loxton et al. (2009) for recent work in this area.

2. PROBLEM FORMULATION

The dynamic behavior of the magnetic-flux profile ψ is described by the following parabolic PDE (Xu et al. (2010)):

$$\frac{1}{\vartheta_1(\hat{\rho})}\frac{\partial \psi}{\partial t}(\hat{\rho}, t) = \frac{u_1(t)}{\hat{\rho}}\frac{\partial}{\partial \hat{\rho}}[\hat{\rho}D(\hat{\rho})\frac{\partial \psi}{\partial \hat{\rho}}(\hat{\rho}, t)] + \vartheta_2(\hat{\rho})u_2(t),$$
(1)

with the Neumann boundary conditions

$$\frac{\partial \psi}{\partial \hat{\rho}}(0, t) = 0, \quad \frac{\partial \psi}{\partial \hat{\rho}}(1, t) = u_3(t), \quad (2)$$

where t denotes time; $\hat{\rho}$ denotes the normalized radius; and $\psi(\hat{\rho}, t)$ denotes the poloidal magnetic flux around the tokamak. Moreover, $\vartheta_1(\hat{\rho})$, $\vartheta_2(\hat{\rho})$, and $D(\hat{\rho})$ are given functions of $\hat{\rho}$ that depend on the particular tokamak device and can be identified offline using experimental data. The auxiliary functions $u_1(t)$, $u_2(t)$ and $u_3(t)$ depend

on the total power P, the total plasma current I, and the average density $\bar{n}$ according to the following equations:

$$u_1(t) = \frac{\bar{n}(t)^{\frac{3}{2}}}{I(t)^{\frac{3}{2}}P(t)^{\frac{3}{4}}}, \ u_2(t) = \frac{P(t)^{\frac{1}{2}}}{I(t)}, \ u_3(t) = kI(t), \ (3)$$

where k is a given constant. Note that $\bar{n}$, I, and P are the control inputs for the physical actuators.

The initial condition for the magnetic flux profile is given by

$$\psi(\hat{\rho}, 0) = \psi_0(\hat{\rho}). \quad (4)$$

The aim is to choose the control inputs $\bar{n}(t), I(t)$ and $P(t)$ so that the output profile $\psi(\hat{\rho}, t)$ is brought as close as possible to the desired target profile $\psi^d(\hat{\rho})$ at $t = T$. Thus, the problem is to minimize the following objective functional:

$$J(\bar{n}, I, P) = \frac{1}{2}\int_0^1 \Gamma_0(\hat{\rho})[\psi(\hat{\rho}, T) - \psi^d(\hat{\rho})]^2 d\hat{\rho}$$
$$+ \int_0^T (\Gamma_1\bar{n}(t) + \Gamma_2 I(t) + \Gamma_3 P(t))\, dt, \quad (5)$$

where $\Gamma_0(\hat{\rho})$ is a non-negative weighting function and Γ_1, Γ_2 and Γ_3 are non-negative weighting factors.

The actuator inputs must satisfy the following physical bound constraints:

$$a_1 \le \bar{n}(t) \le b_1, \ a_2 \le I(t) \le b_2, \ a_3 \le P(t) \le b_3, \quad (6)$$

where a_i and b_i $(i = 1, 2, 3)$ are given constants. Any vector-valued piecewise-continuous function $\boldsymbol{\theta}=[\bar{n}, I, P]^\top :$ $[0, T] \rightarrow \mathbb{R}^3$ that satisfies the bound constraints (6) is called an admissible control. Let Θ denote the class of all such admissible controls.

For notational simplicity, we define $\psi_t(\hat{\rho}, t) = \frac{\partial \psi}{\partial t}(\hat{\rho}, t)$, $\psi_{\hat{\rho}}(\hat{\rho}, t) = \frac{\partial \psi}{\partial \hat{\rho}}(\hat{\rho}, t)$ and $h(\hat{\rho}) = \vartheta_1(\hat{\rho})\vartheta_2(\hat{\rho})$. Then, equation (1) with the boundary conditions (2) and the initial condition (4) can be written as

$$\psi_t(\hat{\rho}, t) = \frac{\vartheta_1(\hat{\rho})u_1(t)}{\hat{\rho}}[\hat{\rho}D(\hat{\rho})\psi_{\hat{\rho}}(\hat{\rho}, t)]_{\hat{\rho}} + h(\hat{\rho})u_2(t), \quad (7a)$$

$$\psi_{\hat{\rho}}(0, t) = 0, \quad \psi_{\hat{\rho}}(1, t) = u_3(t), \quad t \in [0, T], \quad (7b)$$
$$\psi(\hat{\rho}, 0) = \psi_0(\hat{\rho}), \quad \hat{\rho} \in [0, 1]. \quad (7c)$$

We now state our problem formally as follows.

Problem P_0. *Given the PDE system (7), find an admissible control $\boldsymbol{\theta} = [\bar{n}, I, P]^\top \in \Theta$ such that the cost functional (5) is minimized.*

3. FINITE ELEMENT APPROXIMATION

In this section, we apply the Galerkin finite element scheme (Thomée (2006)) to approximate Problem P_0, a distributed parameter optimal control problem, by a sequence of conventional optimal control problems, each governed by a lumped parameter system (Teo and Wu (1984)). An efficient computational algorithm will then be developed in Section 4 for solving these approximate problems.

Let $\eta(\hat{\rho})$ be a trial function. Multiplying both sides of (7a) by $\hat{\rho}\eta(\hat{\rho})$ and then integrating the resulting equation over $[0, 1]$ gives

$$\int_0^1 \hat{\rho}\eta(\hat{\rho})\psi_t d\hat{\rho}$$

$$= u_1(t)\vartheta_1(1)D(1)\eta(1)u_3(t)$$

$$- u_1(t)\int_0^1 [\eta'(\hat{\rho})\vartheta_1(\hat{\rho}) + \eta(\hat{\rho})\vartheta_1'(\hat{\rho})]\hat{\rho}D(\hat{\rho})\psi_{\hat{\rho}}d\hat{\rho} \qquad (8)$$

$$+ u_2(t)\int_0^1 \hat{\rho}h(\hat{\rho})\eta(\hat{\rho})d\hat{\rho}.$$

We partition the spatial domain $[0,1]$ into N equal subintervals $I_i=[\frac{i}{N}, \frac{i+1}{N}]$, $i = 0, 1, \ldots, N-1$. Then, we assume that the magnetic flux $\psi(\hat{\rho}, t)$ can be approximated by a linear combination of the basis B-spline functions $B_i(\hat{\rho})$, $i = 0, 1, 2, \ldots, N$, corresponding to this partition, i.e.,

$$\psi(\hat{\rho}, t) \approx \psi^N(\hat{\rho}, t) = \sum_{i=0}^N X_i(t)B_i(\hat{\rho}), \qquad (9)$$

where $X_i(t), i = 0, 1, \ldots, N$, are weighting functions. By substituting (9) into (8), and choose $\eta(\hat{\rho}) = B_j(\hat{\rho}), j = 0, 1, \ldots, N$, we obtain

$$\sum_{i=0}^N \dot{X}_i(t)\int_0^1 \hat{\rho}B_i(\hat{\rho})B_j(\hat{\rho})d\hat{\rho}$$

$$= u_1(t)\vartheta_1(1)D(1)B_j(1)u_3(t)$$

$$- u_1(t)\sum_{i=0}^N X_i(t)\int_0^1 \hat{\rho}B_i'(\hat{\rho})B_j'(\hat{\rho})\vartheta_1(\hat{\rho})D(\hat{\rho})d\hat{\rho} \qquad (10)$$

$$- u_1(t)\sum_{i=0}^N X_i(t)\int_0^1 \hat{\rho}B_i'(\hat{\rho})B_j(\hat{\rho})\vartheta_1'(\hat{\rho})D(\hat{\rho})d\hat{\rho}$$

$$+ u_2(t)\int_0^1 \hat{\rho}h(\hat{\rho})B_j(\hat{\rho})d\hat{\rho}.$$

We introduce the following notation:

$$A_{ij} = \int_0^1 \hat{\rho}B_i(\hat{\rho})B_j(\hat{\rho})d\hat{\rho}, \qquad (11a)$$

$$\tilde{A}_{ij} = \int_0^1 \hat{\rho}B_i'(\hat{\rho})B_j'(\hat{\rho})\vartheta_1(\hat{\rho})D(\hat{\rho})d\hat{\rho}, \qquad (11b)$$

$$\hat{A}_{ij} = \int_0^1 \hat{\rho}B_i(\hat{\rho})B_j'(\hat{\rho})\vartheta_1'(\hat{\rho})D(\hat{\rho})d\hat{\rho}, \qquad (11c)$$

$$D_j = \int_0^1 \hat{\rho}h(\hat{\rho})B_j(\hat{\rho})d\hat{\rho}, \quad E_j = \vartheta_1(1)D(1)B_j(1), \quad (11d)$$

where $i, j = 0, 1, \ldots, N$. Then equation (10) can be rewritten in matrix form as follows:

$$\mathbf{A}\dot{\mathbf{X}}(t) = -u_1(t)[\tilde{\mathbf{A}} + \hat{\mathbf{A}}]\mathbf{X}(t) + u_2(t)\mathbf{D} + u_1(t)u_3(t)\mathbf{E},$$

where

$$\mathbf{X}(t) = [X_0(t), X_1(t), \ldots, X_N(t)]^\top,$$

$$\mathbf{A} = [A_{ij}], \quad \tilde{\mathbf{A}} = [\tilde{A}_{ij}], \quad \hat{\mathbf{A}} = [\hat{A}_{ij}],$$

$$\mathbf{D} = [D_0, D_1, \ldots, D_N]^\top, \quad \mathbf{E} = [E_0, E_1, \ldots, E_N]^\top.$$

Recalling the initial condition (7c), we have

$$\psi_0(\hat{\rho}) = \sum_{i=0}^N X_i(0)B_i(\hat{\rho}). \qquad (12)$$

We multiply both sides of (12) by $\hat{\rho}B_j(\hat{\rho})$ and then integrate over $[0,1]$ to obtain $\mathbf{AX}(0) = \mathbf{G}$, where $\mathbf{G} = [G_0, G_1, \ldots, G_N]^\top$ and

$$G_j = \int_0^1 \hat{\rho}B_j(\hat{\rho})\psi_0(\hat{\rho})d\hat{\rho}, \quad j = 0, 1, \ldots, N. \qquad (13)$$

By following the same arguments as in Lin et al. (2009), it can be shown that matrix $\mathbf{A}$ is nonsingular. Thus, we have $\mathbf{X}(0) = \mathbf{A}^{-1}\mathbf{G}$.

Consequently, the equations in (7) can be rewritten as

$$\dot{\mathbf{X}}(t) = \mathbf{F}(\mathbf{X}(t), \boldsymbol{\theta}(t))$$

$$= -\frac{\bar{n}(t)^{\frac{3}{2}}}{I(t)^{\frac{3}{2}}P(t)^{\frac{3}{4}}}\mathbf{A}^{-1}[\tilde{\mathbf{A}} + \hat{\mathbf{A}}]\mathbf{X}(t)$$

$$+ \frac{P(t)^{\frac{1}{2}}}{I(t)}\mathbf{A}^{-1}\mathbf{D} + \frac{k\bar{n}(t)^{\frac{3}{2}}}{I(t)^{\frac{1}{2}}P(t)^{\frac{3}{4}}}\mathbf{A}^{-1}\mathbf{E}, \qquad (14a)$$

$$\mathbf{X}(0) = \mathbf{A}^{-1}\mathbf{G}. \qquad (14b)$$

Now, for the desired output profile $\psi^d(\hat{\rho})$, we can also obtain

$$\bar{\mathbf{D}} = \bar{\mathbf{A}}\mathbf{X}^d, \qquad (15)$$

where

$$\bar{A}_{ij} = \int_0^1 B_i(\hat{\rho})B_j(\hat{\rho})d\hat{\rho}, \quad i, j = 0, 1, \ldots, N, \qquad (16)$$

$$\bar{D}_j = \int_0^1 \psi^d(\hat{\rho})B_j(\hat{\rho})d\hat{\rho}, \quad j = 0, 1, \ldots, N. \qquad (17)$$

Using the same arguments as in Lin et al. (2009), it can be shown that matrix $\bar{\mathbf{A}}$ is nonsingular, just like matrix $\mathbf{A}$. Therefore, the coefficients for the desired profile are given by

$$\mathbf{X}^d = \bar{\mathbf{A}}^{-1}\bar{\mathbf{D}}. \qquad (18)$$

Using the expansion (9), the computed output profile $\psi(\hat{\rho}, T)$ at the terminal time T can be approximated as follows:

$$\psi(\hat{\rho}, T) = \sum_{i=0}^N X_i(T)B_i(\hat{\rho}), \qquad (19)$$

where $X_i(T), i = 0, 1, \ldots, N$, are weighting coefficients. Then, the cost functional (5) becomes

$$J(\bar{n}, I, P) = \frac{1}{2}\sum_{i=0}^N \sum_{j=0}^N (X_i(T) - X_i^d)(X_j(T) - X_j^d)$$

$$\times \int_0^1 \Gamma_0(\hat{\rho})B_i(\hat{\rho})B_j(\hat{\rho})d\hat{\rho}$$

$$+ \int_0^T (\Gamma_1\bar{n}(t) + \Gamma_2 I(t) + \Gamma_3 P(t)) dt.$$

Hence, the cost functional (5) can be rewritten as

$$J(\bar{n}, I, P) = \frac{1}{2}[\mathbf{X}(T) - \mathbf{X}^d]^\top \mathbf{M}[\mathbf{X}(T) - \mathbf{X}^d]$$

$$+ \int_0^T (\Gamma_1\bar{n}(t) + \Gamma_2 I(t) + \Gamma_3 P(t)) dt, \qquad (20)$$

where $\mathbf{M} = [M_{ij}]$ and

$$M_{ij} = \int_0^1 \Gamma_0(\hat{\rho})B_i(\hat{\rho})B_j(\hat{\rho})d\hat{\rho}, \quad i, j = 0, 1, \ldots, N.$$

Problem P_0, the distributed parameter optimal control problem, is now approximated by the following conventional parameter optimal control problem, which we call Problem P_N.

Problem $\mathbf{P}_N$. *Given the dynamic system (14), find an admissible control $\boldsymbol{\theta} = [\bar{n}, I, P]^\top \in \Theta$ such that the cost functional (20) is minimized.*

4. OPTIMAL CONTROL COMPUTATION

To solve Problem P_N, we will apply the control parameterization method (Teo et al. (1991)). We subdivide the time horizon $[0, T]$ into p subintervals $[t_{k-1}, t_k), k = 1, 2, \ldots, p$, where $t_k, k = 0, 1, \ldots, p$, are fixed knot points such that

$$0 = t_0 < t_1 < t_2 < \cdots < t_{p-1} < t_p = T. \quad (21)$$

The vector-valued control function $\boldsymbol{\theta} = [\bar{n}, I, P]^\top$ is then approximated by a constant vector on each subinterval:

$$\boldsymbol{\theta}(t) \approx \boldsymbol{\sigma}^k, \ t \in [t_{k-1}, t_k), \ k = 1, 2, \ldots, p, \quad (22)$$

where $\boldsymbol{\sigma}^k = [\sigma_1^k, \sigma_2^k, \sigma_3^k]^\top$. The piecewise-constant approximation (22) can be expressed as follows:

$$\boldsymbol{\theta}(t) \approx \boldsymbol{\theta}^p(t) = \sum_{k=1}^p \boldsymbol{\sigma}^k \chi_{[t_{k-1}, t_k)}(t), \quad (23)$$

where $\chi_{[t_{k-1}, t_k)} : \mathbb{R} \to \mathbb{R}$ is the indicator function defined by

$$\chi_{[t_{k-1}, t_k)}(t) = \begin{cases} 1, & \text{if } t \in [t_{k-1}, t_k), \\ 0, & \text{otherwise.} \end{cases} \quad (24)$$

Recall that the control variables $\bar{n}(t)$, $I(t)$, and $P(t)$ satisfy the bound constraints (6). Thus, it follows that the control parameters σ_i^k $(i = 1, 2, 3, \ k = 1, 2, \ldots, p)$ satisfy

$$a_i \leq \sigma_i^k \leq b_i, \ i = 1, 2, 3, \ k = 1, 2, \ldots, p. \quad (25)$$

We denote $\boldsymbol{\sigma} = [(\boldsymbol{\sigma}^1)^\top, (\boldsymbol{\sigma}^2)^\top, \ldots, (\boldsymbol{\sigma}^p)^\top]^\top$. Define

$$U = \{\boldsymbol{\sigma} \in \mathbb{R}^{3p} : a_i \leq \sigma_i^k \leq b_i, i = 1, 2, 3, \ k = 1, 2, \ldots, p\}.$$

After control parameterization, the dynamic system (14) becomes

$$\dot{\mathbf{X}}(t) = \sum_{k=1}^p \mathbf{F}(\mathbf{X}(t), \boldsymbol{\sigma}^k) \chi_{[t_{k-1}, t_k)}(t), \quad t \in [0, T], \quad (26a)$$

$$\mathbf{X}(0) = \mathbf{A}^{-1}\mathbf{G}. \quad (26b)$$

Let $\mathbf{X}^p(\cdot|\boldsymbol{\sigma})$ denote the solution of system (26) corresponding to $\boldsymbol{\sigma} \in U$. To determine $\mathbf{X}^p(\cdot|\boldsymbol{\sigma})$, we can solve (26) sequentially over the subintervals $[t_{k-1}, t_k), k = 1, 2, \ldots, p$.

Now, the cost functional (20) becomes

$$\mathcal{J}^p(\boldsymbol{\sigma}) = \frac{1}{2}[\mathbf{X}^p(T|\boldsymbol{\sigma}) - \mathbf{X}^d]^\top \mathbf{M}[\mathbf{X}^p(T|\boldsymbol{\sigma}) - \mathbf{X}^d]$$
$$+ \sum_{k=1}^p \left(\Gamma_1 \sigma_1^k + \Gamma_2 \sigma_2^k + \Gamma_3 \sigma_3^k\right)(t_k - t_{k-1}), \quad (27)$$

where $\mathcal{J}^p(\boldsymbol{\sigma}) = J(\boldsymbol{\theta}^p)$. We may now state the approximate optimal parameter selection problem as follows.

Problem $\mathbf{P}_N^p$. *Given the lumped parameter system (26), find a control parameter vector $\boldsymbol{\sigma} \in U$ such that the cost functional (27) is minimized over U.*

Problem P_N^p is an optimal parameter selection problem in the so-called canonical form (Teo et al. (1991)). In principle, such problems can be solved as nonlinear optimization problems using the SQP method. However, to do this, we need the gradient of the cost functional (27) with respect to the decision parameters. Since (27) is only an implicit, rather than explicit, function of $\boldsymbol{\sigma}$, computing its gradient is a non-trivial task. Thankfully this gradient

can be computed using the sensitivity method described in Loxton et al. (2008).

We first define the state variation with respect to σ_i^k as follows:

$$\mathbf{S}^{ki}(t|\boldsymbol{\sigma}) = \frac{\partial \mathbf{X}^p(t|\boldsymbol{\sigma})}{\partial \sigma_i^k}, \ k = 1, 2, \ldots, p, \ i = 1, 2, 3. \quad (28)$$

Furthermore, let

$$\delta_{kl} = \begin{cases} 1, & \text{if } k = l, \\ 0, & \text{otherwise,} \end{cases} \quad \hat{\delta}_{kl} = \begin{cases} 1, & \text{if } k \leq l, \\ 0, & \text{otherwise.} \end{cases}$$

Then, for each $k = 1, 2, \ldots, p$ and $i = 1, 2, 3$, it can be shown (see Loxton et al. (2008)) that the state variation defined in (28) satisfies the following dynamic system:

$$\dot{\mathbf{S}}^{ki}(t) = \hat{\delta}_{kl} \frac{\partial \mathbf{F}(\mathbf{X}^p(t|\boldsymbol{\sigma}), \boldsymbol{\sigma}^l)}{\partial \mathbf{X}} \mathbf{S}^{ki}(t)$$
$$+ \delta_{kl} \frac{\partial \mathbf{F}(\mathbf{X}^p(t|\boldsymbol{\sigma}), \boldsymbol{\sigma}^l)}{\partial \theta_i}, \quad (29)$$
$$t \in [t_{l-1}, t_l), l = 1, 2, \ldots, p,$$

with the initial condition

$$\mathbf{S}^{ki}(0) = \mathbf{0}. \quad (30)$$

As a result, by using the chain rule, we can derive the gradient of $\mathcal{J}^p(\boldsymbol{\sigma})$ as follows:

$$\frac{\partial \mathcal{J}^p(\boldsymbol{\sigma})}{\partial \sigma_i^k} = [\mathbf{X}^p(T|\boldsymbol{\sigma}) - \mathbf{X}^d]^\top \mathbf{M}\mathbf{S}^{ki}(T|\boldsymbol{\sigma})$$
$$+ \Gamma_i(t_k - t_{k-1}), \ k = 1, 2, \ldots, p, \ i = 1, 2, 3. \quad (31)$$

By incorporating these formulae into a nonlinear programming algorithm such as SQP, we can solve Problem P_N^p numerically. See Lin et al. (2014) for more details.

5. NUMERICAL SIMULATIONS

We now apply the proposed computational algorithm to an example. This example, which comes from Xu et al. (2010), is based on experimental data from the DIII-D tokamak in San Diego, California. The functions $D(\hat{\rho})$, $\vartheta_1(\hat{\rho})$, and $\vartheta_2(\hat{\rho})$ in the PDE model (1) are given in reference Xu et al. (2010). The initial magnetic flux profile is taken from shot #129412 from the DIII-D tokamak.

For the spatial discretization of the PDE system, we use the first-order basis functions $B_i(\hat{\rho}), i = 0, 1, \ldots, N$, defined by

$$B_i(\hat{\rho}) = \begin{cases} 1 + N\hat{\rho} - i, & \hat{\rho} \in \left[\dfrac{i-1}{N}, \dfrac{i}{N}\right], \\ 1 - N\hat{\rho} + i, & \hat{\rho} \in \left[\dfrac{i}{N}, \dfrac{i+1}{N}\right], \\ 0, & \text{otherwise,} \end{cases} \quad (32)$$

where $N = 25$ is the number of subintervals in the spatial domain.

In applying the control parameterization technique, we subdivide the time interval $[0, T]$ into p subintervals, with $t_0 = 0$ and $t_p = 1.2$. Note that the approximate controls switch value at the switching instants $t = t_k, k = 1, 2, \ldots, p - 1$. The lower and upper bounds in (6) are given by: $a_1 = 0.1$ [10^{19}m^{-3}], $b_1 = 100.5$ [10^{19}m^{-3}], $a_2 = 0.1$ MA, $b_2 = 100.9$ MA, $a_3 = 0.01$ MW, $b_3 = 10$ MW. Furthermore, the weighting factors in the objective func-
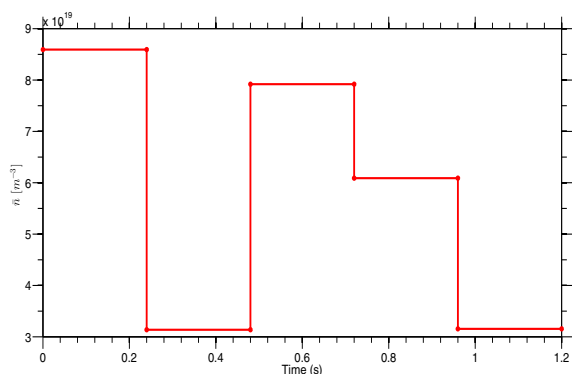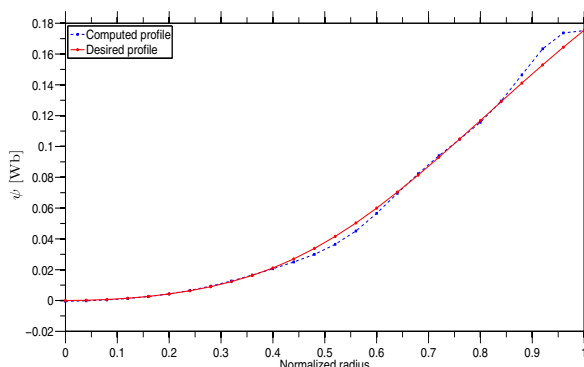
(a) Optimal control input $\bar{n}(t)$.
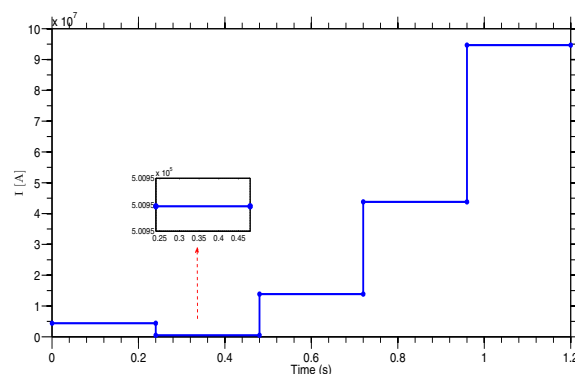
(b) Optimal control input $I(t)$.
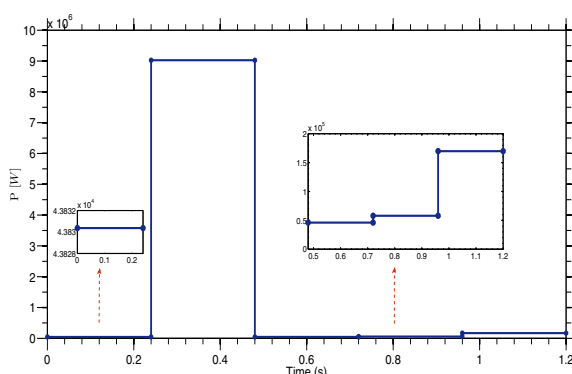
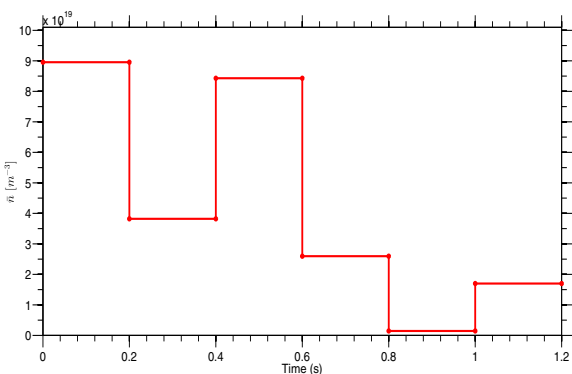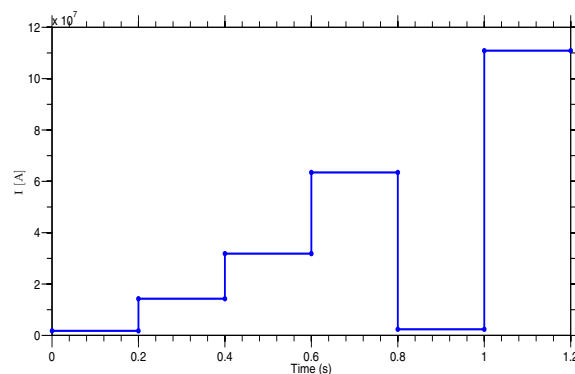(c) Optimal control input $P(t)$.

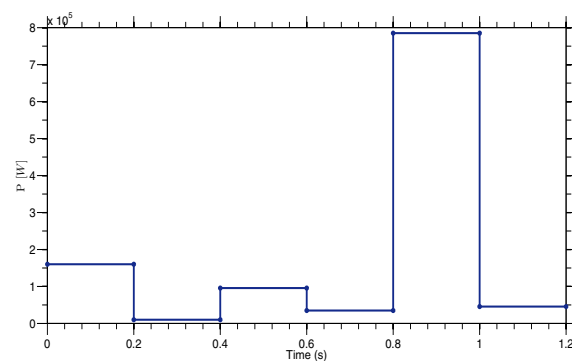(d) Optimal ψ-profile at the terminal time.

Fig. 2. Optimal controls and optimal ψ-profile for $p = 5$.
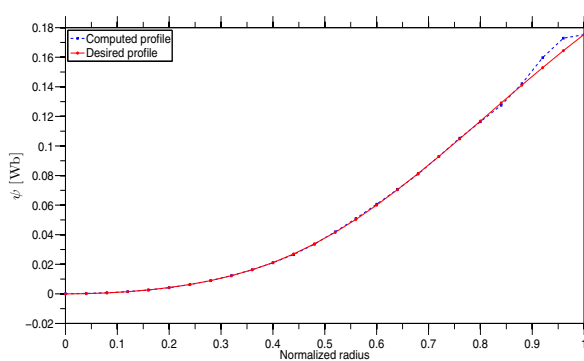

(a) Optimal control input $\bar{n}(t)$.

(b) Optimal control input $I(t)$.

(c) Optimal control input $P(t)$.

(d) Optimal ψ-profile at the terminal time.

Fig. 3. Optimal controls and optimal ψ-profile for $p = 6$.

tional (5) are $\Gamma_1 = 10^{-25}$, $\Gamma_2 = 10^{-12}$, $\Gamma_3 = 10^{-12}$ and

$$\Gamma_0(\hat{\rho}) = \sum_{i=0}^{N} \frac{1}{\sqrt{2\pi\varepsilon}} \exp\left\{-\frac{(\hat{\rho} - \frac{i}{N})^2}{2\varepsilon^2}\right\},$$

where $\varepsilon = 0.4$. This choice for Γ_0 consists of a linear combination of bell curves with peaks at the spatial knot points $\hat{\rho} = i/N$, $i = 0, 1, \ldots, N$. Thus, deviation from the desired target profile is penalized most severely at the spatial knot points in the PDE spatial discretization.

Our numerical simulation study was carried out within the MATLAB programming environment running on a personal computer with the following configuration: Intel Core i7-2600 3.40GHz CPU, 4.00GB RAM, 64-bit Windows 7 Operating System. Our MATLAB code implements the gradient-based optimization procedure described in Section 4 by combining FMINCON with the sensitivity method for gradient computation. We initially used MATLAB's non-stiff differential equation solver ODE45 to integrate the state system (26) and the sensitivity systems (29). However, we noticed that ODE45 struggled to solve the state and sensitivity systems, which indicates that these differential equations are stiff. Hence, we subsequently replaced ODE45 in our code with the stiff solver ODE15s. All of the numerical results presented in this section were generated using ODE15s.

The optimal controls and optimal flux profiles for $p = 5, 6$, are shown in Fig. 2, Fig. 3, respectively. As the control variables change with time, the numerical optimization procedure can drive the final ψ-profile to within close proximity of the predefined desired profile. When p is increased from $p = 5$ to $p = 6$, the simulation results show that the trajectory matching error is reduced, as expected. However, we note that increasing p further from $p = 6$ to $p = 7$ does not result in any significant change in the objective functional value, despite a significant increase in the overall computation time. For example, the computation time for $p = 7$ is almost 40% longer than for $p = 6$, but the improvements in the flux profile and the cost functional are negligible.

6. CONCLUSION

This paper has presented an effective computational method for solving a finite-time optimal control problem arising during the ramp-up phase of tokamak plasmas. The method is based on a combination of the Galerkin finite element and control parameterization methods. Simulation results using experimental data from the DIII-D tokamak demonstrate that the method is effective at driving the plasma profile to a predefined desired profile at the terminal time. Nevertheless, there is still much room for improvement, i.e., we can add path constraints on the control variables in our problem formulation in Section 2, and we can also take the control switching points as decision variables, along with the control heights, by applying the so-called *time-scaling transformation* described in Lin et al. (2014).

REFERENCES

Ariola, M. and Pironti, A. (2008). *Magnetic Control of Tokamak Plasmas*. Springer.

Ariyur, K. and Krstic, M. (2003). *Real-time Optimization by Extremum-seeking Control*. Wiley.

Lin, Q., Loxton, R., and Teo, K.L. (2014). The control parameterization method for nonlinear optimal control: A survey. *Journal of Industrial and Management Optimization*, 10(1), 275–309.

Lin, Q., Wu, Y.H., Loxton, R., and Lai, S.Y. (2009). Linear B-spline finite element method for the improved Boussinesq equation. *Journal of Computational and Applied Mathematics*, 224(2), 658–667.

Loxton, R., Teo, K.L., and Rehbock, V. (2008). Optimal control problems with multiple characteristic time points in the objective and constraints. *Automatica*, 44(11), 2923–2929.

Loxton, R., Teo, K.L., Rehbock, V., and Yiu, K.F.C. (2009). Optimal control problems with a continuous inequality constraint on the state and the control. *Automatica*, 45(10), 2250–2257.

Murakami, M., Wade, M., Greenfield, C., Luce, T., Ferron, J., John, H.S., DeBoo, J., Heidbrink, W., Luo, Y., Makowski, M., et al. (2006). Progress toward fully noninductive, high beta conditions in DIII-D. *Physics of Plasmas*, 13(5), 056106.

Ou, Y., Luce, T., Schuster, E., Ferron, J., Walker, M., Xu, C., and Humphreys, D. (2007). Towards model-based current profile control at DIII-D. *Fusion Engineering and Design*, 82(5), 1153–1160.

Ou, Y., Xu, C., Schuster, E., Ferron, J., Luce, T., Walker, M., and Humphreys, D. (2011). Receding-horizon optimal control of the current profile evolution during the ramp-up phase of a tokamak discharge. *Control Engineering Practice*, 19(1), 22–31.

Ou, Y., Xu, C., Schuster, E., Luce, T., Ferron, J., Walker, M., and Humphreys, D. (2008). Design and simulation of extremum-seeking open-loop optimal control of current profile in the DIII-D tokamak. *Plasma Physics and Controlled Fusion*, 50(11), 115001.

Taylor, T. (1997). Physics of advanced tokamaks. *Plasma Physics and Controlled Fusion*, 39(12B), B47–B79.

Teo, K.L., Goh, C.J., and Wong, K.H. (1991). *A Unified Computational Approach to Optimal Control Problems*. Longman Scientific and Technical.

Teo, K.L. and Wu, Z.S. (1984). *Computational Methods for Optimizing Distributed Systems*. Academic Press.

Thomée, V. (2006). *Galerkin Finite Element Methods for Parabolic Problems*, volume 25. Springer.

Witrant, E., Joffrin, E., Brémond, S., Giruzz, G., Mazon, D., Barana, O., and Moreau, P. (2007). A control-oriented model of the current profile in tokamak plasma. *Plasma Physics and Controlled Fusion*, 49(7), 1075–1105.

Xu, C., Ou, Y., Dalessio, J., Schuster, E., Luce, T., Ferron, J., Walker, M., and Humphreys, D. (2010). Ramp-up phase current-profile control of tokamak plasmas via nonlinear programming. *IEEE Transactions on Plasma Science*, 38(2), 163–173.